Joint Phase Recovery for XPIC System exploiting Adaptive Kalman Filtering

Anna Vizziello, *Member, IEEE,* Pietro Savazzi, *Member, IEEE,* and Roberta Borra

***Abstract*—The phase recovery scheme of a cross-polar interference cancellation (XPIC) system is considered here, assuming two completely independent RF transceiver chains for the two different polarizations. A novel Kalman based algorithm is proposed to jointly recover the phase of both the main polarization signal and the interfering one, at each single receiver of an XPIC system. The time evolution of the received phases and frequencies is represented by using both a new four-state model and a simplified two-state implementation. Simulations are conducted considering a typical backhaul link and the results prove the effectiveness of the proposed solution, compared to a common phase-locked loop (PLL) approach. Unlike the PLL scheme, the proposed Kalman-based algorithm directly adapts its parameters according to the different channel conditions, i.e. the signal-to-noise ratio per bit (E_b/N_0) and the the cross-polarization discrimination (XPD).**

***Index Terms*—Kalman Filter, phase recovery, cross-polar interference cancellation (XPIC), digital microwave, point-to-point wireless, backhaul.**

I. Introduction

Cross Polarization Interference Cancellation (XPIC) technology consists of employing the same carrier frequency for the simultaneous transmission and reception of two independent streams of data, so that the links capacity is doubled without using new spectrum [1].

In this work we consider the implementation of a cross-polarized communications system based on two independent transceiver chains, in order to have the maximum flexibility to connect different single carrier transceivers to dual-polarized antennas [2]. Following this reasoning, the investigated architecture could also be extended to distributed multiple input and multiple output systems, which is envisioned as a powerful enabler technology for 5G system backhaul networks.

We here propose an XPIC receiver which performs carrier phase synchronization by means of an Extended Kalman filter (EKF). It jointly recovers the phase of both the received signal and the interfering one at the input of the cross-polar interference canceller. As far as the authors know, it is the first time that a Kalman approach is applied to XPIC architectures. Some studies consider Kalman solutions for carrier synchronization but only in single-input single-output system (SISO) architectures as in [3] [4].

The main contributions of the paper are both a novel four-state Kalman filter algorithm for an XPIC receiver, and a simplified version of it, which exploits two simpler two-state Kalman filters.

A. Vizziello and P. Savazzi are with the Department of Electrical, Computer and Biomedical Engineering, University of Pavia, via Ferrata 5, Pavia, 27100 Italy e-mail: givenname.surname@unipv.it.

R. Borra is with SIAE Microelettronica, Via Michelangelo Buonarroti 1, Cologno Monzese, MI, 20093 Italy e-mail: roberta.borra@siaemic.com.

Extensive simulations prove the effectiveness of the proposed solution compared with a typical phase-locked loop (PLL) approach. The main benefit of the proposed Kalman-based algorithm is its adaptability to different channel conditions, in terms of signal-to-noise ratio per bit (E_b/N_0) and cross-polarization descrimination (XPD), showing that it is equivalent to a PLL architecture with adaptive filter loop parameters.

The paper is organized as follows: Sec. II describes the system model, Sec. III details the proposed solution for both four-state and two-state models. Sec. IV shows some interesting simulation results, and, finally, some concluding remarks wrap up and close the paper in Sec. V.

II. System Model

The system architecture considers two distinct receivers for the two different polarized signals. Let us consider the signal received at one path $r_0(n)$:

$$r_0(n) = t_0(n)e^{j\theta(n)} + gt_1(n)e^{j\phi(n)} + w(n) \qquad (1)$$

where $t_0(n)$ is the QAM transmitted symbol of the main polarization component, with received phase $\theta(n)$, g is the cross-polar attenuation factor, $t_1(n)$ is the interfering symbol coming from the other polarization path, with phase $\phi(n)$, and $w(n)$ is an additive white Gaussian noise (AWGN) with variance σ_w^2.

The objective of this work is to estimate the phases $\theta(n)$ and $\phi(n)$, along with the corresponding frequencies $\dot{\theta}(n)$ and $\dot{\phi}(n)$, by using a novel four-state Kalman filtering algorithm. The input of the main polarization slicer is:

$$u_0(n) = \left(r_0(n) - gt_1(n)e^{-j\hat{\phi}(n)}\right) e^{-j\hat{\theta}(n)} \qquad (2)$$

where $\hat{\phi}(n)$ and $\hat{\theta}(n)$ represent the estimated phases of the main and cross polar signals at the receiver.

In this model we do not take into account multipath fading effects, that is equivalent to consider the signal $r_0(n)$ at the output of an equalizer, which typically is a linear minimum mean square error (MMSE) one. Following the same reasoning, the multiplication by the coefficient g could be replaced by a discrete convolution, considering a linear MMSE canceler with a filter length greater than 1.

The above hypothesis corresponds to assume ideal equalization and interference cancellation, which means assuming the canceller gain g to be known. This is equivalent to consider the fast varying phase $\phi(n)$ tracked by the cross PLL or by the Kalman algorithm, while the canceller converges to a static, or slow varying, phase error.

$$\mathbf{H}(n)=\begin{bmatrix} -\hat{a}(n)\sin(\hat{\theta}(n|n-1))-\hat{b}(n)\cos(\hat{\theta}(n|n-1)) & 0 & 0 & 0 \\ -\hat{b}(n)\sin(\hat{\theta}(n|n-1))+\hat{a}(n)\cos(\hat{\theta}(n|n-1)) & 0 & 0 & 0 \\ 0 & 0 & -\hat{c}(n)\sin(\hat{\theta}(n|n-1))-\hat{d}(n)\cos(\hat{\theta}(n|n-1)) & 0 \\ 0 & 0 & -\hat{d}(n)\sin(\hat{\theta}(n|n-1))+\hat{c}(n)\cos(\hat{\theta}(n|n-1)) & 0 \end{bmatrix} \tag{11}$$

III. Joint Phase recovery based on Extended Kalman Filtering

A. The Four-State Modeling Approach

The model state vector is defined as:

$$\mathbf{x}(n)=\begin{bmatrix} \theta(n) \\ \dot{\theta}(n) \\ \phi(n) \\ \dot{\phi}(n) \end{bmatrix} \tag{3}$$

for which the state evolution results:

$$\mathbf{x}(n)=\mathbf{F}\mathbf{x}(n-1)+\mathbf{s}(n) \tag{4}$$

where $\mathbf{s}(n)$ in the state noise, while the transition matrix $\mathbf{F}$ is defined as

$$\mathbf{F}=\begin{bmatrix} 1 & 1 & 0 & 0 \\ 0 & 1 & 0 & 0 \\ 0 & 0 & 1 & 1 \\ 0 & 0 & 0 & 1 \end{bmatrix} \tag{5}$$

Exploiting (1), the observation vector $\mathbf{r}(n)$ can be expressed as a non-linear function $\mathbf{h}(\mathbf{x}(n)) \doteq \mathbf{h}(n)$:

$$\mathbf{r}(n)=\mathbf{h}(n)+\mathbf{w}(n) \tag{6}$$

where:

$$\mathbf{r}(n)=\begin{bmatrix} Re(\tilde{r}_0(n)) \\ Im(\tilde{r}_0(n)) \\ Re(gt_1(n)) \\ Im(gt_1(n)) \end{bmatrix},\ \mathbf{h}(n)=\begin{bmatrix} Re(\hat{t}_0(n)e^{j\theta(n)}) \\ Im(\hat{t}_0(n)e^{j\theta(n)}) \\ Re(g\hat{t}_1(n)e^{j\phi(n)}) \\ Im(g\hat{t}_1(n)e^{j\phi(n)}) \end{bmatrix} \tag{7}$$

$\mathbf{w}(n)$ is the observation noise, $\hat{t}_0(n)=\hat{a}(n)+j\hat{b}(n)$ is the output of the symbol detector, $\tilde{r}_0(n)=r_0(n)-gt_1(n)e^{-j\hat{\phi}(n)}$, and:

$$g\hat{t}_1(n)e^{j\phi(n)}=r_0(n)-\hat{t}_0(n)e^{j\theta(n)}=\hat{c}(n)+j\hat{d}(n) \tag{8}$$

Let us define $\hat{\mathbf{x}}(n|k)$ as the estimation of $\mathbf{x}(n)$ at time n, given the observation state vector $\mathbf{r}(i)$ with $i=1,2,...,k$. In order to use the EKF, we employ the first order linearization method to $\mathbf{h}(\mathbf{x}(n))$ around the estimation of the state vector $\hat{\mathbf{x}}(n|n-1)$ as follows:

$$\mathbf{h}(\mathbf{x}(n))=\hat{\mathbf{x}}(n|n-1)+\frac{\delta\mathbf{h}}{\delta\mathbf{x}}|_{\mathbf{x}=\hat{\mathbf{x}}(n|n-1)}(\mathbf{x}(n)-\hat{\mathbf{x}}(n|n-1)) \tag{9}$$

where

$$\mathbf{H}(n)=\frac{\delta\mathbf{h}}{\delta\mathbf{x}}|_{\mathbf{x}=\hat{\mathbf{x}}(n|n-1)} \tag{10}$$

Specifically, the computation of (10), shown in (11), uses the estimated symbols $\hat{t}_0(n)$ also for obtaining $\hat{c}(n)+j\hat{d}(n)$ by (8). In this way, the four-state decision-directed (DD) EKF algorithm can be divided in the following two steps:

1) Measurements update equations: where we calculate the conditional mean $\hat{\mathbf{x}}(n|n)$ of the state vector $\hat{\mathbf{x}}(n)$, the Kalman gains $\mathbf{K}(n)$, and the variance $\mathbf{R}(n|n)$ of the state vector $\hat{\mathbf{x}}(n)$ at time instant n, according to (12), (13), and (14) respectively:

$$\hat{\mathbf{x}}(n|n)=\hat{\mathbf{x}}(n|n-1)+\mathbf{K}(n)[\mathbf{r}(n)-\mathbf{h}(n)] \tag{12}$$

$$\mathbf{K}(n)=\mathbf{R}(n|n-1)\mathbf{H}^H(n)[\mathbf{H}(n)\mathbf{R}(n|n-1)\mathbf{H}^H(n)+\mathbf{Q}_w]^-1 \tag{13}$$

where $\mathbf{Q}_w$ is the covariance matrix of the noise $\mathbf{w_n}$,

$$\mathbf{R}(n|n)=[\mathbf{I}-\mathbf{K}(n)\mathbf{H}(n)]\mathbf{R}(n|n-1) \tag{14}$$

2) Time update equations: in which we calculate the conditional mean $\hat{\mathbf{x}}(n+1|n)$ and variance $\mathbf{R}(n+1|n)$ of the state vector $\hat{\mathbf{x}}(n)$ at the update time instant $n+1$, according to (15) and (16) respectively:

$$\hat{\mathbf{x}}(n+1|n)=\mathbf{F}\hat{\mathbf{x}}(n|n) \tag{15}$$

$$\mathbf{R}(n+1|n)=\mathbf{F}\mathbf{R}(n|n)\mathbf{F}^H+\mathbf{Q}_s \tag{16}$$

where $\mathbf{Q}_s$ is the covariance matrix of the noise $s(n)$.

B. The Two-State Modeling Approach

The two-state vectors of the main and cross polar signal are expressed as

$$\mathbf{x}_0(n)=\begin{bmatrix} \theta(n) \\ \dot{\theta}(n) \end{bmatrix} \tag{17}$$

$$\mathbf{x}_1(n)=\begin{bmatrix} \phi(n) \\ \dot{\phi}(n) \end{bmatrix} \tag{18}$$

The state evolution of the linearized Kalman filter results:

$$\mathbf{x}_0(n)=\begin{bmatrix} \theta(n) \\ \dot{\theta}(n) \end{bmatrix}=\mathbf{F}\begin{bmatrix} \theta(n-1) \\ \dot{\theta}(n-1) \end{bmatrix} \tag{19}$$

and

$$\mathbf{x}_1(n)=\begin{bmatrix} \phi(n) \\ \dot{\phi}(n) \end{bmatrix}=\mathbf{F}\begin{bmatrix} \phi(n-1) \\ \dot{\phi}(n-1) \end{bmatrix} \tag{20}$$

where

$$\mathbf{F}=\begin{bmatrix} 1 & 1 \\ 0 & 1 \end{bmatrix} \tag{21}$$

Similarly, the observation vectors $\mathbf{r}_0(n)$ and $\mathbf{r}_1(n)$ are defined as in the following:

$$\begin{aligned} \mathbf{r}_0(n)&=\mathbf{h}_0(\mathbf{x}_0(n))+\mathbf{w}_0(n) \\ \mathbf{r}_1(n)&=\mathbf{h}_1(\mathbf{x}_1(n))+\mathbf{w}_1(n) \end{aligned} \tag{22}$$

$$\mathbf{H}_0(n) = \begin{bmatrix} -\hat{a}(n)\sin(\hat{\theta}(n|n-1)) - \hat{b}(n)\cos(\hat{\theta}(n|n-1)) & 0 \\ -\hat{b}(n)\sin(\hat{\theta}(n|n-1)) + \hat{a}(n)\cos(\hat{\theta}(n|n-1)) & 0 \end{bmatrix}$$
$$\mathbf{H}_1(n) = \begin{bmatrix} -\hat{c}(n)\sin(\hat{\theta}(n|n-1)) - \hat{d}(n)\cos(\hat{\theta}(n|n-1)) & 0 \\ -\hat{d}(n)\sin(\hat{\theta}(n|n-1)) + \hat{c}(n)\cos(\hat{\theta}(n|n-1)) & 0 \end{bmatrix} \quad (25)$$

where $\mathbf{h}_0$ and $\mathbf{h}_1$ are:

$$\mathbf{h}_0(\mathbf{x}_0(n)) = \hat{\mathbf{x}}_0(n|n-1) + \frac{\delta \mathbf{h}_0}{\delta \mathbf{x}_0}|_{\mathbf{x}_0=\hat{\mathbf{x}}_0(n|n-1)} (\mathbf{x}_0(n) - \hat{\mathbf{x}}_0(n|n-1))$$
$$\mathbf{h}_1(\mathbf{x}_1(n)) = \hat{\mathbf{x}}_1(n|n-1) + \frac{\delta \mathbf{h}_1}{\delta \mathbf{x}_1}|_{\mathbf{x}_1=\hat{\mathbf{x}}_1(n|n-1)} (\mathbf{x}_1(n) - \hat{\mathbf{x}}_1(n|n-1)) \quad (23)$$

with

$$\mathbf{H}_0(n) = \frac{\delta \mathbf{h}_0}{\delta \mathbf{x}_0}|_{\mathbf{x}_0=\hat{\mathbf{x}}_0(n|n-1)}$$
$$\mathbf{H}_1(n) = \frac{\delta \mathbf{h}_1}{\delta \mathbf{x}_1}|_{\mathbf{x}_1=\hat{\mathbf{x}}_1(n|n-1)} \quad (24)$$

According to (23) and (24), the matrix $\mathbf{H}_0(n)$ and $\mathbf{H}_1(n)$ are the linearization of $\mathbf{h}_0$ and $\mathbf{h}_1$, respectively. The computation of $\mathbf{H}_0(n)$ and $\mathbf{H}_1(n)$ is shown in (25).

The EKF algorithm described by equations (12)-(16) is applied to both $\mathbf{x}_0(n)$ and $\mathbf{x}_1(n)$, representing respectively the main and the cross-polar signal state vectors.

IV. Simulation Results

A. Simulation Environment

The simulation environment consists of a typical scenario for a 1024-QAM backhaul link, considering phase noise on both main and cross-polar signals, and a frequency offset on the main polarization transmitter. The symbol rate is 25 MHz and the phase noise model at the receiver, which corresponds to the sum of all the transmit and receive oscillator phase noise contributions, is based on the following parameters:

- -67 dBc/Hz at 10 KHz;
- -96 dBc/Hz at 100 KHz.

These phase noise parameters and the E_b/N_0 are used to compute the covariance matrices $\mathbf{Q}_s$ and $\mathbf{Q}_w$ for the Kalman algorithms and the PLL loop gains [5]. The other simulation parameters are specified in the following, according to the different simulation conditions.

B. Performance Evaluation

Simulations have been conducted to evaluate the bit error rate (BER) of the proposed Kalman based solution, considering the four-state model and its simplified two-state version, as well as a more common solution based on two second-order PLLs, for the two phases of the main and cross polar signals to be recovered. Moreover, the cumulative distribution function (CDF) of errors bursts has been evaluated for the four-state Kalman based solution and the PLL ones.

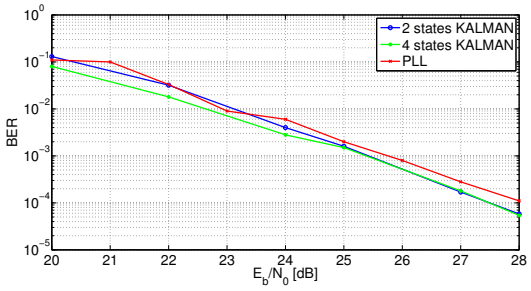

Fig. 1. BER versus E_b/N_0: Kalman and PLL based solutions, 1024-QAM.

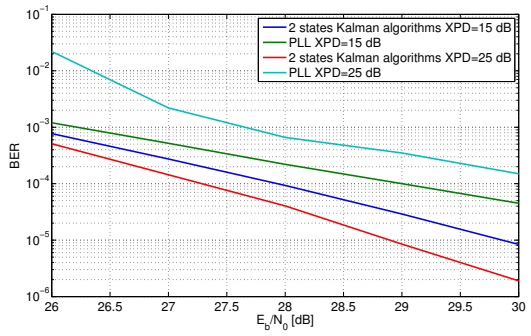

Fig. 2. BER versus E_b/N_0: both the PLL and Kalman (2 states) parameters are optimized for E_b/N_0=26dB and XPD=15dB).

For higher-order M-QAM modulations, it is very common to aid the phase noise filtering process by using pilot tones, i.e. known symbols are periodically inserted. In the rest of the paper we have considered the periodical transmission of known constellation points [6]. A pilot tone, i.e. a known corner symbol, is transmitted every 55 symbols and it is used at the main polarization slicer as a periodic perfect decision, and to periodically force the correct phase value for both the Kalman and PLL algorithms.

1) BER performance: Fig. 1 shows the BER versus the E_b/N_0. The figure refers to a 1024-QAM modulation scheme, where the classical PLL solution has been compared to the two versions of the proposed Kalman based algorithm. As shown in Fig. 1, Kalman based solutions perform slightly better than the PLL based one, with the further advantage that the Kalman phase tracker corresponds to a second-order PLL with automatic gain optimizations.

In order to show this important property of the proposed Kalman scheme, the BER curves in Fig. 2 compare the performance of the two schemes when both the PLL and the Kalman parameters are optimized under the following channel conditions: E_b/N_0 = 26 dB, XPD = 15 dB. It can be seen

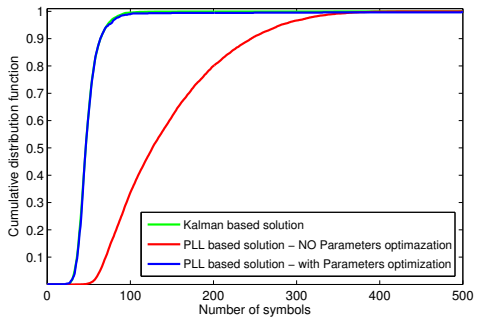

Fig. 3. Cumulative distribution function of error bursts (1024 QAM, E_b/N_0=22dB, XPD=25dB).

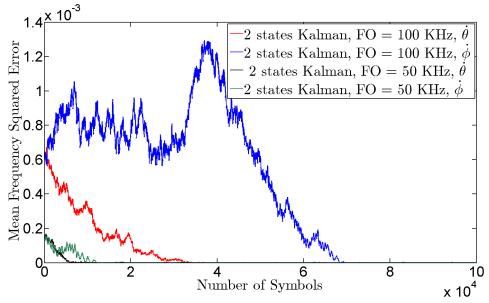

(a) Kalman performance

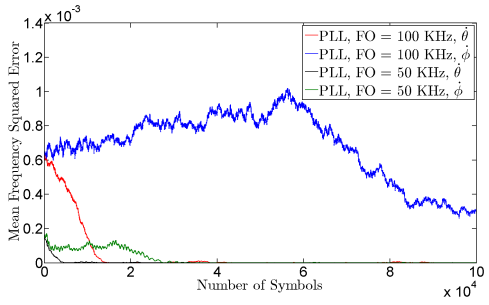

(b) PLL performance

Fig. 4. Mean Frequency Squared Error, E_b/N_0=28 dB, XPD=15dB

that the PLL performance with fixed parameters is very poor compared to the Kalman one. It is interesting to further note that the Kalman performs better when XPD = 25 dB, despite its parameters have been computed for XPD = 15 dB. This proves that the Kalman algorithm is less sensitive to XPD variations and the performance is better since the interference power is lower. On the contrary the PLL results are very poor when XPD = 25 dB since the cross PLL loop gains are optimized for a different level of the interference power. The main PLL parameters have been computed using the well-known closed-form solutions [5], where the cross-polar one has been optimized by a heuristic search procedure. Moreover, the parameters for both Kalman and PLL schemes are set accordingly to the given phase noise model, since the local oscillator phase noise does not change significantly over time.

2) CDF of error bursts: here, we consider error bursts that can happen when employing the different investigated architectures, and calculate their error CDF, assuming a window with a length of 500 symbols and an overlapping factor of 250 symbols.

Specifically, Fig. 3 refers to the case of a PLL scheme with and without optimization of the loop filter gains, in order to show the difference with respect to the Kalman filter which is adaptive in nature. In more details, the PLL loop filter gains in the worst case have been optimized for $E_b/N_0 = 29$ dB, while the simulated $E_b/N_0 = 22$ dB, emulating a mismatched parameter setting.

When impairments at the oscillators are only due to presence of phase noise, as in the results shown in in Fig. 1-3, the convergence period of the two techniques is comparable, and corresponds to a few tens of symbols.

3) Mean Frequency Squared Error: Fig. 4 shows that the Kalman algorithm provides better results, since $\hat{\dot{\phi}}(n)$ converges more rapidly with respect to the PLL case, as outlined by the blue and green curves. Once the two algorithms converge, the BER performance is comparable with the results shown previously. In order to get good symbol decisions at the output of the receiver, both the estimated frequencies $\hat{\dot{\theta}}(n)$, $\hat{\dot{\phi}}(n)$ shall converge.

V. Conclusion

In this work we have considered a cross-polarized communications system based on two independent transceiver chains, in order to have the maximum flexibility to connect different single carrier transceivers to dual-polarized antennas.

A new four-state Kalman algorithm for tracking both the received symbol phase and the interferer one has been proposed. Simulations results prove the effectiveness of the proposed solution in terms of BER performance and robustness against frequency offset, compared to a common second-order PLL.

Furthermore, a low-burden implementation exploiting two simpler Kalman schemes has been investigated, providing a comparable performance with the four-state complete algorithm. One further benefit of the proposed solutions is that they directly adapt their parameters to the new channel conditions, corresponding to a variable-gain PLL.

References

[1] Noel, P.; Klemes, M., "Doubling the through-put of a Digital Microwave Radio system by the implementation of a cross-polarization interference cancellation algorithm," *Radio and Wireless Symposium (RWS)*, 2012 IEEE , vol., no., pp.363,366, 15-18 Jan. 2012.

[2] L. Rossi, N. Calia, M. Nava, C. Salvaneschi, P. Agabio, B. Cornaglia, A. Ratia, "2xSTM-1 Frequency Reuse System with XPIC," *in Proc. 8th European Conference on Fixed Wireless Networks and Technologies, ECRR 2007*, Paris, April 3-5, 2007.

[3] Campeanu, A.; Gal, J., "Kalman filter carrier synchronization algorithm," *Electronics and Telecommunications (ISETC)*, 2012 10th International Symposium on , vol., no., pp.203,208, 15-16 Nov. 2012.

[4] Wei-Tsen Lin; Dah-Chung Chang, "Adaptive Carrier Synchronization Using Decision-Aided Kalman Filtering Algorithms," *Consumer Electronics, IEEE Transactions on* , vol.53, no.4, pp.1260,1267, Nov. 2007.

[5] A. Spalvieri, M. Magarini, "Wiener's Analysis of the Discrete-Time Phase-Locked Loop With Loop Delay," *IEEE Trans. on Circuits And Systems*, Vol. 55, No. 6, Jun. 2008.

[6] A. Spalvieri, L. Barletta, "Pilot-Aided Carrier recovery in The Presence of Phase Noise," *IEEE Trans. Comm.*, Vol. 59, No. 7, Jul. 2011.